The Journal of Neuroscience, February 15, 2002, 22(4):1328–1337

Activity Deprivation Reduces Miniature IPSC Amplitude by Decreasing the Number of Postsynaptic $GABA_A$ Receptors Clustered at Neocortical Synapses

Valerie Kilman, Mark C. W. van Rossum, and Gina G. Turrigiano

Department of Biology and Center for Complex Systems, Brandeis University, Waltham, Massachusetts 02454

Maintaining the proper balance between excitation and inhibition is necessary to prevent cortical circuits from either falling silent or generating epileptiform activity. One mechanism through which cortical networks maintain this balance is through the activity-dependent regulation of inhibition, but whether this is achieved primarily through changes in synapse number or synaptic strength is not clear. Previously, we found that 2 d of activity deprivation increased the amplitude of miniature EPSCs (mEPSCs) onto cultured visual cortical pyramidal neurons. Here we find that this same manipulation decreases the amplitude of mIPSCs. This occurs with no change in single-channel conductance but is accompanied by a reduction in the average number of channels open during the mIPSC peak and a reduction in the intensity of staining for $GABA_A$ receptors ($GABA_A$Rs) at postsynaptic sites. In addition, the number of synaptic sites that express detectable levels of $GABA_A$Rs was decreased by ~50% after activity blockade, although there was no reduction in the total number of presynaptic contacts. These data suggest that activity deprivation reduces cortical inhibition by reducing both the number of $GABA_A$Rs clustered at synaptic sites and the number of functional inhibitory synapses. Because excitatory and inhibitory synaptic currents are regulated in opposite directions by activity blockade, these data suggest that the balance between excitation and inhibition is dynamically regulated by ongoing activity.

Key words: synaptic plasticity; activity-dependent; mIPSC; $GABA_A$ receptor; synapse elimination; nonstationary fluctuation analysis

Cortical circuits are highly recurrent and are prone to instability when the balance between excitation and inhibition is perturbed (Kriegstein et al., 1987; Chagnac-Amitai et al., 1989). This raises the question of how this balance is maintained during periods of development when the number and strength of synapses are changing dramatically. One mechanism by which cortical networks prevent runaway excitation is by scaling the strength of all excitatory connections up or down as a function of how active they are (Turrigiano, 1999; Turrigiano and Nelson, 2000). Synaptic scaling occurs in part through changes in the number of glutamate receptors clustered at synaptic sites, which produces an increase or decrease in quantal amplitude (Lissen et al., 1998; O'Brien et al., 1998; Turrigiano et al., 1998; Watt et al., 2000). This form of synaptic plasticity is slow, requiring hours to days of altered activity to produce changes in synaptic strength, and scales up or down proportionally all excitatory synapses (Turrigiano et al., 1998).

Inhibition can also be regulated by long-lasting changes in activity. In primate and rodent visual cortex, visual deprivation or inhibition of retinal activity with TTX can decrease immunoreactivity for GABA (Hendry and Jones, 1986, 1988; Benevento et al., 1995). A similar phenomenon has been demonstrated in cortical and hippocampal cultures, in which activity blockade reversibly decreases GABA immunoreactivity (Marty et al., 1996; Rutherford et al., 1997) and reduces the amount of functional inhibition received by pyramidal neurons (Rutherford et al., 1997). In addition to regulating the number of GABA-immunopositive neurons, activity blockade can modulate the number of inhibitory synaptic contacts received by cultured Purkinje and hippocampal neurons (Seil and Drake-Baumann, 1994, 2000; Marty et al., 2000). Finally, epilepsy paradigms have been shown to decrease the amplitude and frequency of some classes of miniature IPSCs (mIPSCs) (Wierenga and Wadman, 1999) and to regulate the number of postsynaptic $GABA_A$ receptors ($GABA_A$R) clustered at synaptic sites (Otis et al., 1994; Nusser et al., 1998).

These studies raise the possibility that inhibitory synaptic strengths, like excitatory synaptic strengths, can be scaled up or down by long-lasting changes in activity. To directly test this idea, we recorded mIPSCs from pyramidal neurons after blocking all spiking activity with TTX for 2 d. Whereas activity blockade scales up the strength of mEPSCs (Lissen et al., 1998; O'Brien et al., 1998; Rutherford et al., 1998; Turrigiano et al., 1998; Watt et al., 2000), here we find that this same manipulation scales mIPSC amplitudes down. This reduction in quantal amplitude was accompanied by a reduction in the number of open $GABA_A$R channels and in the intensity of staining for $GABA_A$Rs at synaptic sites. In addition, the number of postsynaptic sites that localized $GABA_A$Rs decreased, although overall synaptic density remained unchanged. These data indicate that the quantal amplitude of excitatory and inhibitory synapses are regulated in opposite directions by activity blockade and suggest that the

Received March 28, 2001; revised Nov. 6, 2001; accepted Nov. 27, 2001.

This work was supported by National Science Foundation Grant IBN 9726944 and National Institutes of Health Grant RO1 NS36853. G.G.T. was supported by Career Development Award K02 NS01893. We are grateful for many helpful discussions with Sacha Nelson and for technical assistance from S. Moore and T. Casimiro.

Correspondence should be addressed to Gina G. Turrigiano, Department of Biology, MS 08, Brandeis University, 415 South Street, Waltham, MA 02454. E-mail: turrigiano@brandeis.edu.

V. Kilman's present address: Department of Neurobiology and Physiology, Northwestern University, Evanston, IL 60201.

balance between excitatory and inhibitory synaptic strengths is dynamically regulated by ongoing activity.

MATERIALS AND METHODS

Cell cultures. Dissociated cell cultures were prepared from postnatal day 3 (P3) to P5 Long–Evans rat pups as described previously (Rutherford et al., 1997; Watt et al., 2000), except that neurons were plated onto confluent astrocyte beds plated onto glass-bottomed dishes. Neuronal medium contained 2% B27 supplement (Invitrogen, Gaithersburg, MD). Cultures were used after 8–10 d *in vitro*. On each of the 2 d immediately before use, half of the dishes in a set of cultures were treated with 0.4 μM TTX, whereas the other half were left untreated. All data were obtained in parallel from TTX-treated and age-matched sister control cultures.

Physiology. Recordings were obtained as described previously (Rutherford et al., 1997, 1998; Turrigiano et al., 1998; Watt et al., 2000). Briefly, cultures were placed on the stage of a Nikon (Tokyo, Japan) inverted microscope and perfused with room temperature artificial CSF containing 1 μM TTX, 25 μM CNQX, and 50 μM APV (brought to 320 mOsm with dextrose, bubbled with 5% CO_2–95% O_2). Patch pipettes (3–5 MΩ) were filled with internal electrode solution containing (in mM): 120 $KMetSO_4$, 20 KCl, 10 K-HEPES, 2 $MgSO_4$, 0.5 mM EGTA, and 3 ATP, pH 7.4 with KOH (280 mOsm with sucrose). Junction potentials of ~5 mV were left uncompensated. Whole-cell voltage-clamp recordings were obtained from morphologically identified pyramidal somata (Rutherford et al., 1997; Watt et al., 2000) with an Axopatch 1D or 200B amplifier (Axon Instruments, Foster City, CA). Criteria for accepting a recording included V_m of at least −55 mV, series resistance (R_s) of ≤20 MΩ, R_{in} of ≥200 MΩ, and <10% change in these parameters in the course of recording. For control cells, average $V_m = -59.8 \pm 2.2$ mV, $R_{in} = 588 \pm 95$ MΩ, $R_s = 12.2 \pm 1.4$ MΩ, and whole-cell capacitance of 23.3 ± 3.8 pF; TTX-treated neurons were not significantly different from control neurons in any of these parameters. Spontaneous mIPSCs were recorded by holding cells in voltage clamp at −80 mV. The calculated reversal potential for Cl^- with these internal and external solutions is −49 mV, resulting in inward mIPSCs. These currents were reversibly blocked by bath application of 20 μM bicuculline. In a second series of experiments, $KMetSO_4$ was replaced with KCl in the internal solution to give a symmetrical internal and external chloride concentration, and mIPSCs were recorded at −70 mV. In-house software was used to detect and measure mIPSCs using an amplitude cutoff of 5 pA (Rutherford et al., 1998; Turrigiano et al., 1998; Watt et al., 2000). Multiple events that overlapped, or events with poor baselines, were excluded. To generate the average mIPSC for each neuron, all events recorded from that neuron were aligned on the rising phase and averaged. To generate the average mIPSC for a given experimental condition, the average mIPSC for each neuron recorded in that condition were averaged. The sensitivity of the postsynaptic cell to GABA was assayed by application of pulses of 50 μM GABA through a patch pipette (1.5 μm diameter) using a picospritzer (10 msec at 10 psi). GABA was delivered directly to the soma from a distance of 20 μm.

Fluctuation analysis was used to determine whether the observed changes in the current were mediated by a change in the number of open channels or by a change in the unitary conductance, using standard methods (Traynelis et al., 1993; De Koninck and Mody, 1994; Otis et al., 1994; Auger and Marty, 1997). The single-channel conductance was extracted from the relationship between the variance in the current across mIPSCs and the mean current. The miniature events had a widely varying range of amplitudes, but the decay kinetics were quite uniform across events. Because variations in amplitude will contaminate the estimate of variance attributable to channel closings, the individual events have to be scaled such that their peak amplitude equals the average peak amplitude (Traynelis et al., 1993; De Koninck and Mody, 1994). Peak-scaled fluctuation analysis yields estimates of the single-channel conductance and the number of open channels. This contrasts to fluctuation analysis without peak scaling, which yields the single-channel conductance and both the number of available channels and the open probability.

Immunocytochemistry. Cultures were fixed for at least 20 min in a solution of 4% paraformaldehyde and 5% sucrose in 0.1 M phosphate buffer (PB) pH 7.4. After rinsing three times in PB, nonspecific staining was blocked and the membranes were permeablized with a 20 min incubation in 0.1% Triton X-100 in PB with 10% goat normal serum added (PB-GNS). Primary antisera diluted in PB-GNS were applied to the cultures for at least 2 hr at room temperature or overnight at 4°C (this procedure was modified slightly for one of the antibodies; see below). After several rinses in PB, secondary antisera diluted in PB-GNS were similarly applied. For double-label experiments, both primaries were applied simultaneously, as were both secondaries. After a final series of PB rinses, glass coverslips were applied with Fluoromount-G.

Antibodies. Three primary antisera were used. A rabbit polyclonal affinity-purified antiserum against synapsin I (AB1543P; Chemicon, Temecula, CA) recognizes all brain synaptic terminals and was used at a dilution of 1:800. A monoclonal antibody generated in mouse against glutamic acid decarboxylase (GAD) (1522 825; Boehringer Mannheim, Indianapolis, IN) specifically recognizes GAD65, the synaptically localized isoform of the synthetic enzyme for GABA. This antibody was used at a dilution of 1:200. A pan-$GABA_AR$ β chain monoclonal antibody generated in mouse (MAB341; Chemicon) was used at a dilution of 1:5. For this antibody, the blocking solution was modified to contain 0.2% Triton X-100 in PB with 20% GNS and 0.1% bovine serum albumin added (PB-GNS-BSA), and the primary diluent was PB-GNS-BSA.

Secondary antisera generated in goat against either mouse or rabbit IgG were labeled with Texas Red or FITC and were diluted 1:50–1:100. For most experiments, Texas Red-tagged goat anti-rabbit IgG marked synapsin, whereas FITC-tagged goat anti-mouse IgG marked the GAD65 or $GABA_AR$ staining. In a few experiments, the opposite fluorescent labels were used (e.g., FITC-tagged goat anti-rabbit), with no obvious differences in the results. For experiments on enhanced green fluorescent protein (EGFP)-labeled cells, Texas Red-tagged secondaries were used for all primary antisera. Control experiments with no primary antiserum, or with the incorrect species secondary, resulted in no specific staining.

Transfection with enhanced green fluorescent protein. To fill the entire dendritic tree of a small number of neurons, cultures were transfected with EGFP using a Bio-Rad (Hercules, CA) gene gun. A plasmid containing DNA for EGFP under a constitutive viral promoter was the kind gift of Dr. L. Griffith (Brandeis University). The plasmid DNA was isolated using standard techniques (Maxi-prep kit; Qiagen, Hilden, Germany). The DNA was then $CaCl_2$ precipitated onto 0.6 μM gold beads (microcarriers) at a ratio of 2 μg of DNA per milligram of gold. The microcarriers were loaded into polyvinyl chloride tubing "bullets" (0.25 mg/bullet). These bullets were used in the Bio-Rad gene gun, which forces the DNA microcarriers off the walls of the tubing with a high-pressure (110 psi) burst of nitrogen gas. A small number of cells in each dish (up to 15) are hit by a microcarrier and express the DNA, which labels entire neuronal arbors with EGFP. Maximal expression was obtained within 24 hr. We shot cultures 24 hr before use and then processed for immunocytochemistry as usual.

Photography and image analysis. Before image collection, the dishes were coded to conceal treatment condition, while also allowing a pair of treated and control dishes to be collected at each microscope session. All data collection and analysis were done blind to experimental condition. Cultures were viewed on an inverted Olympus Optical (Tokyo, Japan) IX70 microscope equipped with fluorescein and rhodamine optics, using a 60× oil immersion lens, numerical aperture of 1.25. Digital photographs were taken with a SenSys cooled CCD camera (PhotoMetrics Inc., Huntington Beach, CA) and Openlab software (Improvision Inc., Lexington, MA). The exposure time and image bit range for each stain were fixed within an experiment to allow comparison between conditions.

Cultures in which random dendrites were examined were all double labeled for synapsin and either GAD65 or $GABA_AR$. Three to six dishes per condition (control or TTX treated) were examined for several replications of each experiment. Four to eight 34 × 45 μm pictures were taken in each dish, one per quadrant. Regions selected had small-diameter dendrites (<5 μm), well spaced to allow accurate counting. To control bleaching and selection bias of the GAD65 and $GABA_AR$ labeling, the synapsin staining for a selected region was scanned and quickly photographed, and only then was the staining for the other label examined and photographed. EGFP-transfected cultures were used to examine the apical-like dendrites of pyramidal neurons. These cultures were also immunocytochemically labeled with either synapsin or GAD65. Photography of the dendrite began at the distal tip and progressed proximally. Bleaching was minimized by photographing large fields (70–135 μm^2) and by first focusing on the EGFP-labeled dendrite and then switching filters just before photographing the second label.

Apical-like dendrites were also examined from untransfected neurons in cultures double labeled for $GABA_AR$ and synapsin. Pyramidal neurons were selected based on anatomical criteria as described below, but with the additional constraint that the soma and at least 100 μm of the apical dendrite needed to be recognizable from background staining and

unobscured by overlying cells. Photography of these apicals began at the most distal portion clearly belonging to the selected pyramidal and progressed proximally to the soma. Digital images were quantified with Openlab software (Improvision Inc.). Dendrites were traced from EGFP labeling or from background staining in unlabeled dendrites. Puncta stained by synapsin, GAD65, or $GABA_ARs$ were selected based on a fixed intensity difference from local background intensity. For each selected punctum, both the area and maximum intensity were measured.

RESULTS

Experiments were performed on dissociated cultures from primary visual cortex of P3–P5 rat pups, after 8–10 d *in vitro*. These cultures contain both excitatory pyramidal neurons and inhibitory GABAergic interneurons, which form extensive synaptic interconnections and develop spontaneous activity after a few days in culture (Rutherford et al., 1997; Turrigiano et al., 1998). All physiological and anatomical data were obtained from neurons with a pyramidal morphology (teardrop-shaped somata with a broad apical-like dendrite and generally symmetric basilar dendrites). Neurons with this morphology are immunonegative for GABA (Rutherford et al., 1997) and form excitatory glutamatergic synaptic connections with other neurons (Rutherford et all, 1998; Turrigiano et al., 1998; Watt et al., 2000).

Activity deprivation reduces mIPSC amplitude

To test the idea that mIPSC amplitude is modified by activity blockade, whole-cell voltage-clamp recordings were obtained from pyramidal neurons grown either in control medium or medium supplemented with TTX for 2 d before recording. mIPSCs were recorded in the presence of TTX, CNQX, and APV (to block spike-mediated transmission and mEPSCs). Neurons were voltage clamped at −80 mV with a chloride reversal potential of −49 mV, so mIPSCs were recorded as inward currents (Fig. 1*a*), which were completely blocked by 20 μM bicuculline (data not shown). Treatment with TTX produced a shift in the distribution of mIPSCs toward smaller-amplitude values (Fig. 1*b*). The average amplitude of mIPSCs decreased to 60.9% of control values after TTX treatment, from −19.7 ± 2.6 to −12.0 ± 0.8 pA (n = 9 neurons in each condition; TTX significantly different from control; p = 0.02) (Fig. 2*a*,*b*). As reported previously (Rutherford et al., 1997, 1998; Turrigiano et al., 1998; Desai et al., 1999; Watt et al., 2000), TTX treatment had no significant effects on the passive properties of the neurons. In addition, the kinetics of the mIPSCs were not significantly different between control and TTX-treated neurons, as can be seen from the scaled average mIPSCs (Fig. 2*a*, *Scaled Average*). Individual measurements of rise times (control, 2.1 ± 0.3 msec; TTX, 2.5 ± 0.2 msec) and decay times (control, 22.8 ± 2.0 msec; TTX, 22.6 ± 1.4 msec) revealed no significant differences between conditions. The reversal potential was close to the calculated chloride reversal potential of −49 mV (control, −48.4 ± 3.6 mV; TTX, −47.7 ± 3.4 mV; n = 7 and 6, respectively) and was not different between control and TTX-treated neurons (Fig. 2*c*).

mIPSC frequency is decreased by TTX treatment

To increase our resolution of small events and measure mIPSC frequencies more accurately, we recorded a second data set from a holding potential of −70 mV with a chloride reversal potential of 0 mV. In this data set, as above, TTX treatment for 2 d significantly reduced mIPSC amplitude (control, −44.5 ± 4.7 pA; TTX, −29.9 ± 4.9 pA; n = 10 and 8, respectively; $p < 0.05$). The frequency of mIPSCs was also reduced by TTX treatment from 0.32 ± 0.04 to 0.17 ± 0.03 Hz ($p < 0.02$).

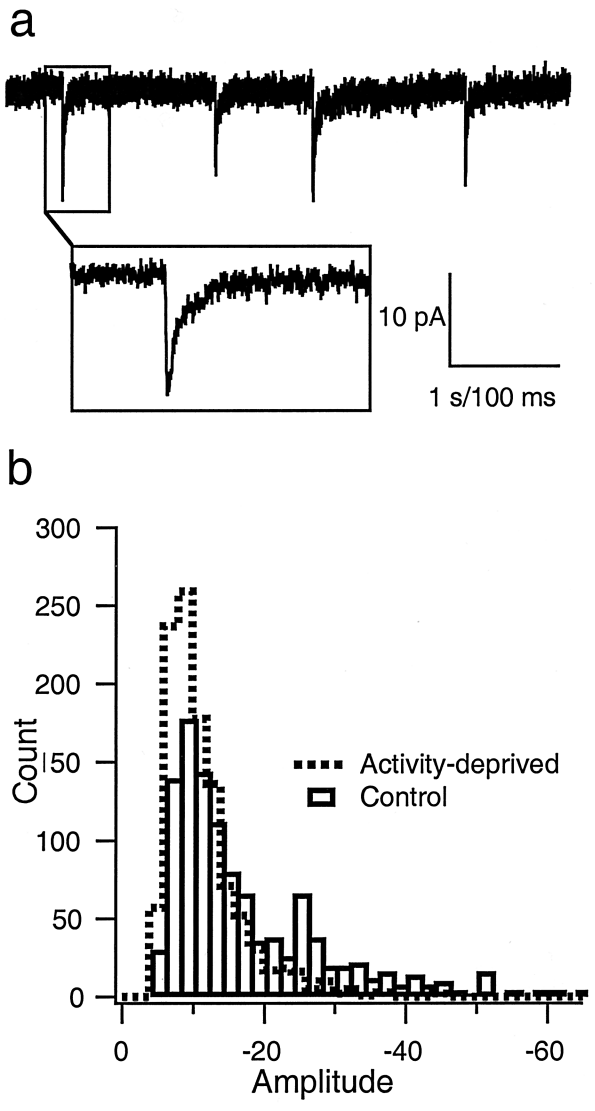

Figure 1. mIPSCs. *a*, An example of mIPSCs recorded as inward currents from a holding potential of −80 mV. *Inset* shows the time course of one event. Calibration: 1 sec for the *top trace*; 100 msec for *inset*. *b*, Distribution of mIPSC amplitudes recorded from neurons grown in control medium (*Control*; *open bars*) or in medium supplemented with TTX (*Activity-deprived*; *dashed line*) for 2 d before recording. Data were pooled from nine neurons in each condition (30 events per neuron).

Nonstationary fluctuation analysis indicates that single-channel conductance is not affected by TTX treatment

The reduction in mIPSC amplitude could be attributable to a decrease in the single-channel conductance (γ) of $GABA_ARs$ or to a reduction in the number of open channels (N_o). To distinguish between these possibilities, we performed peak-scaled nonstationary fluctuation analysis on the mIPSC currents to derive the single-channel conductance values (Treynalis et al., 1993; De Koninck and Mody, 1994; Otis et al., 1994; Auger and Marty, 1997). Because of the increased signal-to-noise ratio for mIPSCs recorded under conditions of symmetrical chloride, we performed the noise analysis primarily on this data set (n = 8 and 7 for control and TTX-treated neurons, respectively). For each neuron, the mIPSCs were averaged, and individual mIPSCs were peak scaled to the average amplitude (Fig. 3*A*). Plots of mean

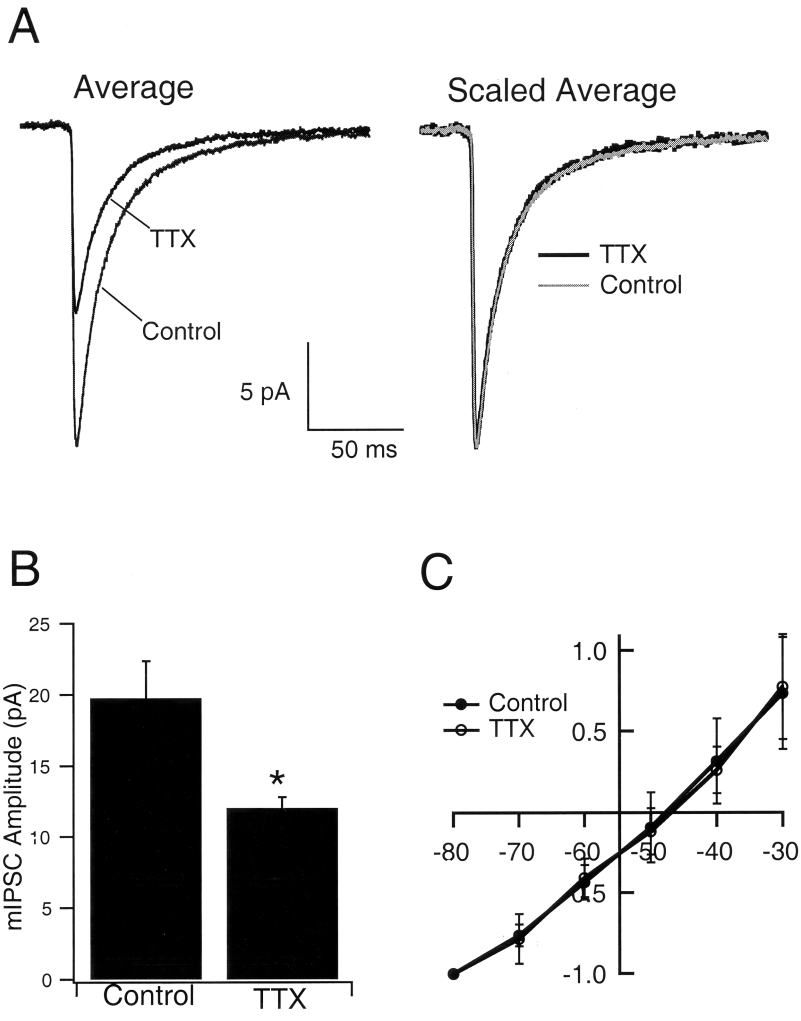

Figure 2. Activity blockade reduces mIPSC amplitude. *A*, *Average*, The average mIPSC from pyramidal neurons grown in control medium or medium supplemented with TTX for 2 d. *Scaled Average*, The average mIPSCs were scaled to the same peak value and overlaid. *B*, Same data set as in *A*; the average mIPSC amplitude for neurons grown in the two conditions. TTX is significantly different from control ($p = 0.02$; $n = 9$ neurons in each condition). *C*, The reversal potential for mIPSCs from neurons grown under the two conditions. Amplitudes were scaled to the values obtained at −80 mV and averaged across neurons grown under the same condition.

variance against mean current (in 200 μsec bins) were well fit by a parabolic function (Fig. 3*B*). The variance of the current σ^2 depends on the mean current μ as follows (Traynelis et al., 1993): $\sigma^2 = \sigma^2_B + i_0\mu - \mu^2/N_0$.

A fit of the data yields the single-channel current i_0, the number of channels that contributed to the mIPSC, N_0, and the background noise σ^2_B. From i_0, the single-channel conductance γ can be calculated. For control neurons, γ was 32.8 ± 7.7 pS, and TTX treatment produced no significant change in the estimate of γ (25.5 ± 6.1 pS; not significantly different from control; $p = 0.58$). These values of γ are close to previously reported values of 20–35 pS for estimates of γ derived from noise analysis and single-channel recordings (Angelotti and Macdonald, 1993; Traynelis et al., 1993; Macdonald and Olsen, 1994; Otis et al., 1994; Auger and Marty,1997). In contrast, there was a significant decrease in N_o after TTX treatment, from 34.7 ± 5.8 to 15.5 ± 4.0 ($p < 0.02$) (Fig. 3*C*). Similar values (34.4 ± 7.1 for control and 14.3 ± 2.6 for TTX) were obtained by dividing (for each neuron) the conductance at the peak of the average mIPSC by the estimated single-channel conductance. These data indicate that the average number of $GABA_AR$ channels open at the peak of the mIPSC is reduced in activity-deprived neurons.

Quantification of $GABA_AR$ and GAD65 immunoreactivity at synaptic sites

The reduction in mIPSC amplitude, coupled with the reduction in N_o, suggests that the number of postsynaptic $GABA_AR$s may be reduced after activity blockade. To test this possibility, we measured the peak fluorescence intensity of $GABA_AR$ labeling at synaptic sites, as well as the density of $GABA_AR$ puncta along dendritic structures. In addition, we quantified the peak fluorescence intensity of labeling for GAD65, the presynaptically localized isoform of the synthetic enzyme for GABA (Kaufman et al., 1991), and the density of GAD65-immunoreactive dendritic puncta. Figure 4*A* shows an example of the colocalization of synapsin, a marker of both excitatory and inhibitory presynaptic terminals (*red*), and GAD65 (*green*) staining, with colocalization shown in *yellow*. All punctate GAD65 staining was colocalized with synapsin. In Figure 4*B*, the culture was stained using antibodies against synapsin (*red*) and a pan-β subunit $GABA_AR$ antibody (*green*). We chose to localize the β chain because all $GABA_AR$s appear to contain a β subunit, whereas α subunit composition varies widely across synapse types (Sieghart, 1995; Dunning et al., 1999). Receptor labeling in this example is primarily synaptic; however, in general, ~20% of punctate $GABA_AR$ staining was nonsynaptic. Synaptic and nonsynaptic $GABA_AR$ puncta were analyzed separately.

In some experiments, we wanted to selectively examine synapses onto pyramidal neurons. We used two methods to accomplish this. First, cultures were transfected at very low efficiency (1–15 neurons per dish) with EGFP, which fills the dendrites of an individual neuron. Cultures were then stained for synapsin or GAD65, which allowed the density of synaptic contacts onto

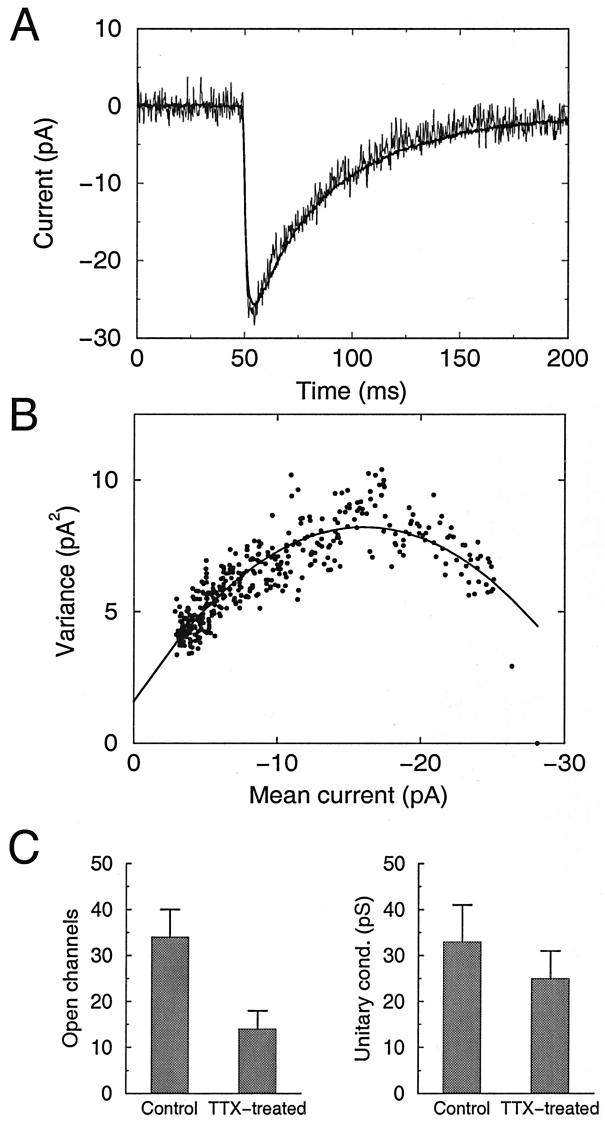

Figure 3. Nonstationary fluctuation analysis of mIPSCs indicates that single-channel conductance is unaffected by activity blockade. *A*, Representative example of the average mIPSC from a control neuron (*smooth line*) and an overlay of a peak-scaled individual mIPSC (*noisy line*), showing the fluctuations about the mean current. *B*, Fluctuation analysis of the neuron shown in *A*. Plot of variance in mIPSC current about the mean current at different times after the peak (*circles*). *Line* shows parabolic fit of the relationship. *C*, Estimates of the number of open channels (*left*) and average single-channel conductance (*right*) for control and TTX-treated neurons. $n = 8$ and 7 for control and TTX-treated neurons, respectively.

individual neurons to be determined. An EGFP-transfected pyramidal neuron is shown in Figure 4*C*, and Figure 4*D* shows one of its EGFP-filled dendrites labeled against synapsin.

Not all punctate $GABA_AR$ staining is localized to synaptic sites. Because we wanted to examine changes in synaptic receptor staining specifically, it was necessary to study $GABA_AR$ staining of pyramidal neurons from cultures colabeled with synapsin. For these experiments, we double-labeled cultures against synapsin and $GABA_ARs$ and selected pyramidal neurons with proximal apical-like dendrites that could be distinguished using background staining. Figure 4, *E* and *F*, shows an example of one such neuron (synapsin, *red*; $GABA_AR$, *green*). Both synaptic and nonsynaptic receptor clusters can be seen in Figure 4*F*.

For all EGFP-filled pyramidal neurons and pyramidal apical dendrites examined, we quantified each punctum (area, intensity, and number) contiguous with or overlying the apical dendrite, and 10–18 neurons were quantified per condition. In addition, we measured the total apical dendritic branch length of EGFP-filled pyramidal neurons from control and activity-deprived cultures.

Intensity of synapsin, $GABA_ARs$, and GAD65 staining after activity blockade

Examples of EGFP-filled dendrites stained against synapsin from control (Fig. 5*A1*) and TTX-treated (Fig. 5*A2*) cultures are shown. The intensity of synapsin staining was similar for both conditions. Figure 5*B1* shows $GABA_AR$ (*green*) and synapsin (*red*) labeling of a pyramidal dendrite from a control culture. In *B2*, $GABA_AR$ staining of the same dendrite is shown in *black* and *white*. *C1* and *C2* are comparable images from a TTX-treated culture. Comparing *B2* with *C2* (following identical and minimal image processing) shows that the $GABA_AR$ staining is less intense in the activity-blocked condition. These dendritic regions are representative of staining under the two conditions, because the average intensity of the puncta in each image was approximately equal to the average for that condition.

The intensity of GAD65 staining of puncta contacting activity-deprived pyramidal apical dendrites was also reduced compared with puncta contacting control neurons. Figure 5, *D1* and *D2*, shows GAD65 staining from a control culture, whereas *E1* and *E2* show a TTX-treated culture. The average intensity of these puncta is near the average for the condition, and the *black* and *white* images in *D2* and *E2* were processed identically.

The intensity of synapsin, $GABA_AR$, and GAD65 immunoreactivity is quantified in Figure 6, for data taken from either random fields of view (*Random dendrites*; three to five repetitions of each experiment; see Materials and Methods) or from pyramidal apical dendrites (*Apical dendrites*; 10–18 neurons per condition). The intensity of synapsin staining was slightly but not significantly increased by activity blockade (Fig. 6*A*). In contrast, the intensity of both GAD65 and synaptically localized $GABA_AR$ staining was significantly reduced after activity blockade (Fig. 6*A*). The intensity of nonsynaptic $GABA_AR$ immunoreactivity was also examined, and, although the effect of TTX treatment was similar in magnitude to that for the synaptically localized receptors, the reduction was not statistically significant. The reduction in intensity of $GABA_AR$ staining after TTX treatment was ~20% when intensity values were not corrected for background fluorescence (Fig. 6) (see Fig. 8). If values were first corrected for the average background fluorescence, then the reduction in intensity was ~31%. These data indicate that both presynaptic expression of the synthetic enzyme for GABA and postsynaptic expression of synaptically localized $GABA_ARs$ are reduced after activity deprivation.

Length density of synapsin, $GABA_ARs$, and GAD65 puncta

The reduction in mIPSC frequency reported above suggests that the number of postsynaptic sites clustering $GABA_ARs$ may be reduced. To investigate this possibility, we quantified the length density (puncta per micrometer of dendritic length) for synapsin, $GABA_AR$, and GAD65 puncta. The density of synapsin puncta was on average 2.1 puncta/10 μm and was unaffected by activity blockade (Fig. 6*B*), and the average number of synapsin puncta per apical dendrite was also unchanged (control, 152 ± 68; TTX, 162 ± 59). The density of GAD65 puncta was also unaffected by

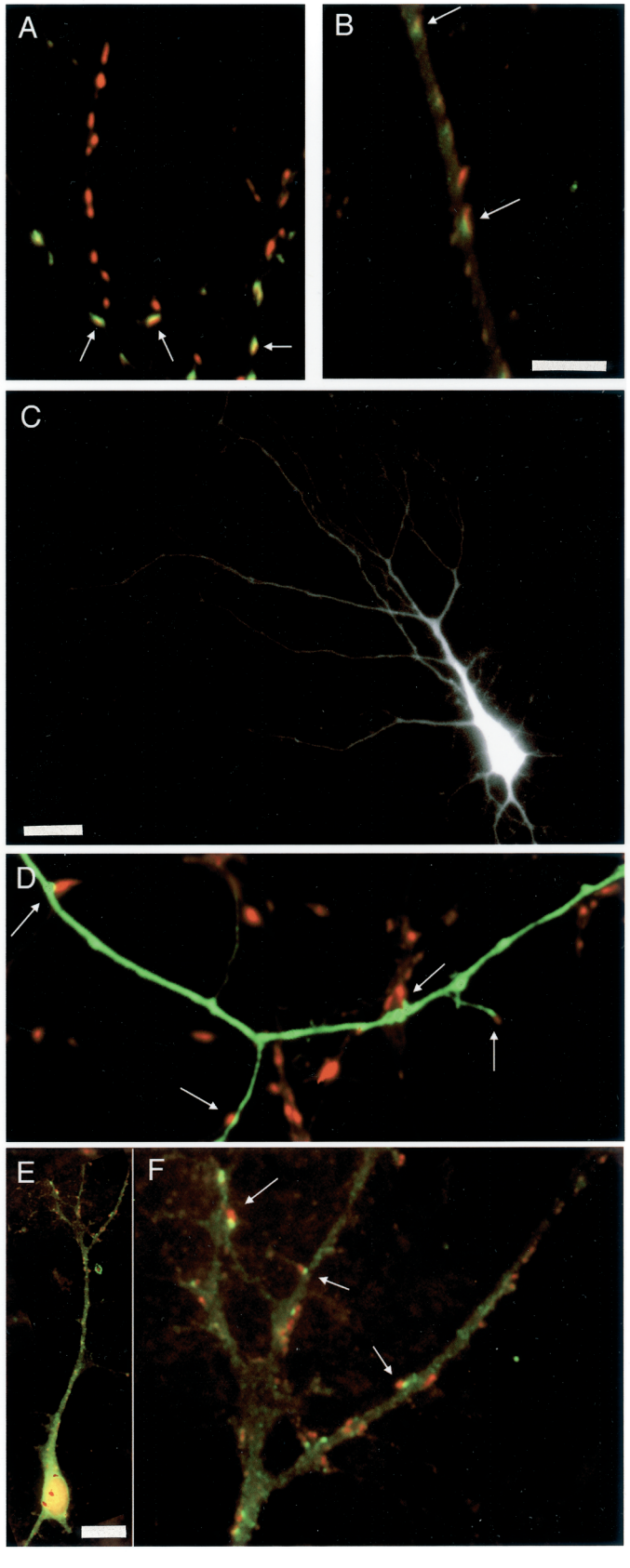

Figure 4. Immunocytochemical labeling of synapsin, GAD65, and $GABA_AR$, and EGFP transfection. *A*, Dendrites stained against synapsin (*red*) and GAD65 (*green*), with double-labeled puncta shown in *yellow*. *B*, Dendrite stained against synapsin (*red*) and $GABA_ARs$ (*green*), with overlap shown in *yellow*. *C*, Apical dendritic arbor of a pyramidal neuron transfected with EGFP. *D*, High-magnification image of the neuron in *C*, showing EGFP-labeled dendrites and immunocytochemical labeling of synapsin (in *red*). *E*, Pyramidal neuron double-labeled for synapsin (*red*) and $GABA_AR$ (*green*). *F*, Higher-magnification view of the apical dendrite shown in *E*. Scale bars: *A*, *B*, *D*, *F*, 5 μm; *C*, 25 μm; *E*, 15 μm. *Arrows* indicate colabeling of puncta (*A*, *B*, *F*) or synapses made onto the EGFP-filled dendrite (*C*).

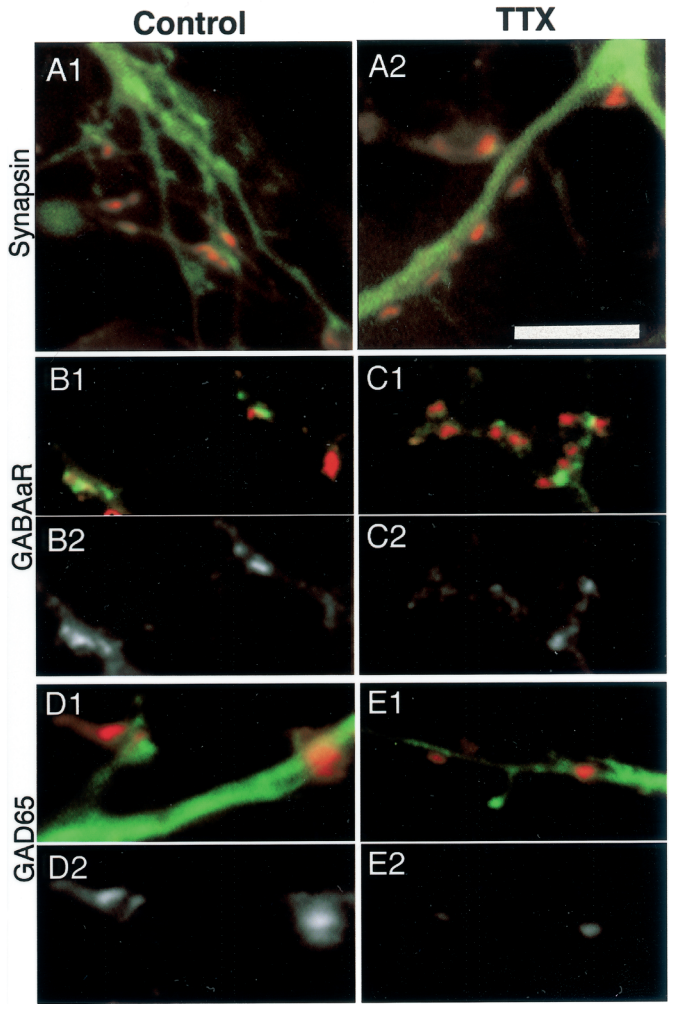

Figure 5. Intensity of *I*mmunofluorescent labeling against synapsin, GAD65, and $GABA_AR$ in control (*left*) and TTX-treated (*right*) cultures. Minimal image processing was used for these illustrations. *Black* and *white* images were photographed with the same exposures and image-processed identically. *A1*, *A2*, The intensity of staining of synapsin puncta (*red*) onto EGFP-labeled dendrites (*green*) does not differ with TTX treatment. *B1*, $GABA_AR$ (*green*) and synapsin (*red*) labeling of a pyramidal apical dendrite, control condition. *B2*, $GABA_AR$ labeling of the dendrite in *B1*, shown in *black* and *white*. *C1*, *C2*, Staining as in *B1* and *B2* for a pyramidal neuron from a TTX-treated culture. $GABA_AR$ labeling is less intense in TTX-treated cultures. *D1*, GAD65 staining (*red*) of EGFP-labeled apical dendrites (*green*), control condition; *D2*, GAD65 labeling of the dendrite in *D1*, shown in *black* and *white*. *E1*, *E2*, Staining as in *D1* and *D2* for a TTX-treated culture. GAD65 staining is also less intense in TTX-treated cultures. Scale bar, 5 μm.

activity blockade in measurements from random dendrites. Measurements onto pyramidal apicals showed a reduction of GAD length density, but this effect was not significant ($p = 0.21$) (Fig. 6*B*). In contrast, the length density of $GABA_AR$ puncta was significantly reduced by activity blockade, by ~25% in measure-

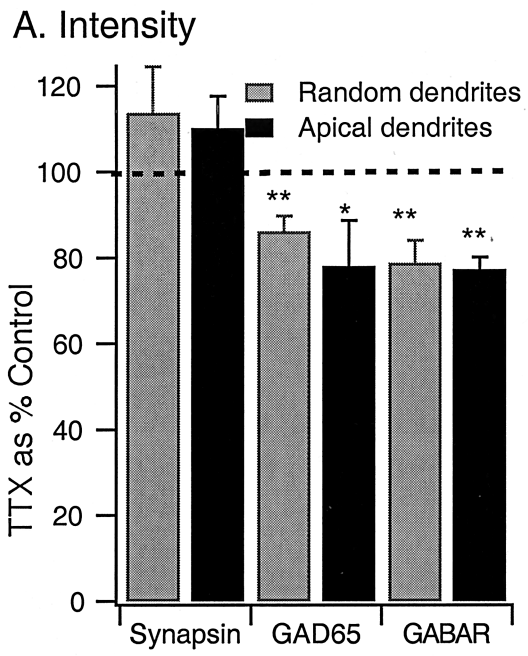

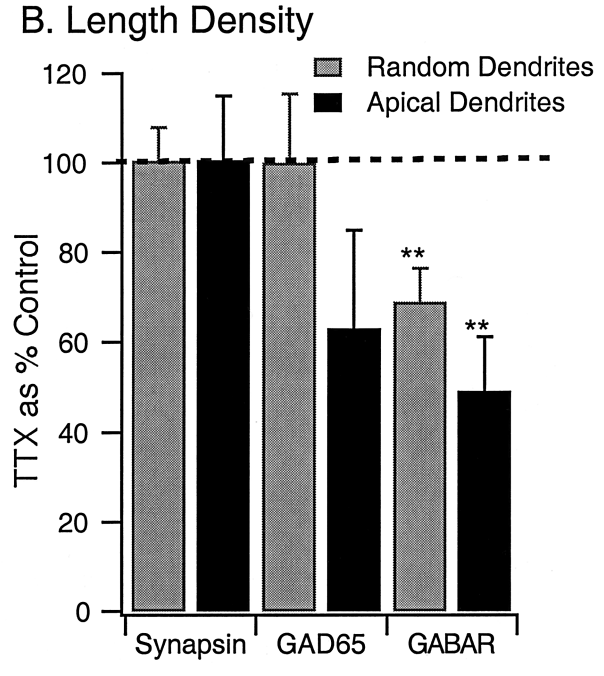

Figure 6. Fluorescent intensity of $GABA_AR$ labeling and the density of synaptic $GABA_AR$ puncta are reduced by activity blockade. *A*, Intensity of labeling of puncta for synapsin, GAD65, and $GABA_AR$, from randomly selected dendritic regions (*Random dendrites*) or from pyramidal apical dendrites (*Apical dendrites*). *B*, Length density (number of immunoreactive puncta per unit length of dendrite) of puncta immunoreactive for synapsin, GAD65, or $GABA_AR$. Data are expressed as a percentage of control; *dashed line* indicates control (100%). $^*p < 0.03$; $^{**}p < 0.01$.

ments from random dendrites and by 50% in measurements onto pyramidal apical dendrites (from 1.2 to 0.6 puncta/10 μm; $p < 0.01$) (Fig. 6*B*). The larger reduction in length density onto pyramidal apicals than onto random dendrites is consistent with a selective effect of activity on inhibitory synapses onto pyramidal neurons.

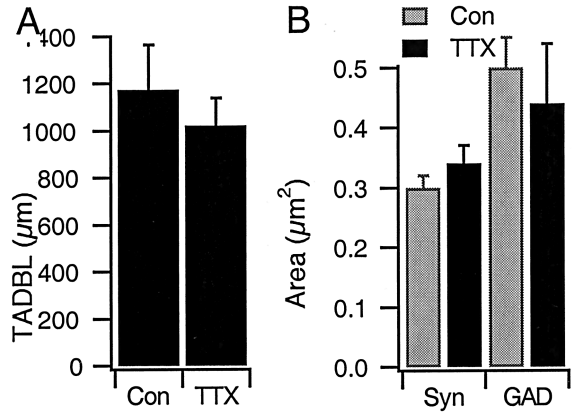

Figure 7. Total apical dendritic branch length and the area of immunoreactive puncta are not affected by activity blockade. *A*, Average total length of the apical-like dendrite from EGFP-filled pyramidal neurons grown under control conditions (*Con*) or in TTX for 2 d before fixation and quantification; $n = 21$ and 12 for control and TTX-treated neurons, respectively. *B*, Average area of puncta immunolabeled for GAD65 or for synapsin (*Syn*), for contacts onto EGFP-filled pyramidal apical dendrites. None of the differences between conditions are statistically significant.

There was no significant change in the total apical dendritic branch length between control EGFP-filled pyramidals and those grown in TTX for 2 d ($n = 21$ and 12 control and TTX-treated neurons, respectively; $p = 0.58$) (Fig. 7*A*). In addition, there was no significant effect of activity blockade on the area of synaptic puncta (Fig. 7*B*). Together, these data indicate that the overall density of presynaptic terminals remains constant after activity blockade but that the number of postsynaptic sites that express detectable levels of $GABA_ARs$ are dramatically reduced.

Consistent with a general reduction in the number of postsynaptic $GABA_AR$ clusters and the intensity of staining within remaining clusters, we found that direct application of GABA to the postsynaptic neuron evoked smaller currents in TTX-treated neurons than in control neurons. GABA was applied to the soma as described previously for glutamate-activated currents (Turrigiano et al., 1998; Watt et al., 2000) while recording in the presence of TTX, CNQX, and APV. TTX treatment produced a large and significant reduction in the amplitude of GABA-evoked currents, to 37.8 ± 14% of control values (TTX significantly different from control; $p < 0.04$; $n = 9$ in each condition).

mIPSC amplitude and $GABA_AR$ intensity scale multiplicatively in response to activity blockade

A plot of the cumulative distribution of mIPSC amplitudes was generated by randomly selecting and combining 30 events per neuron for both the control and TTX-treated conditions ($n = 9$ neurons for each condition) (Fig. 8*a*). TTX treatment shifted the entire distribution of amplitudes to the left, toward smaller values. Activity blockade produces a multiplicative increase in the amplitude of mEPSC amplitudes (Turrigiano et al., 1998). To determine whether the reduction in mIPSC amplitude is also multiplicative, we plotted the rank-ordered control values against the rank-ordered TTX values. The resulting relationship was well fit by a straight line ($r = 0.99$), with a slope of 0.46 and an intercept of 7.5. Transforming the control distribution by this equation resulted in a very good fit to the TTX data (Fig. 8*a*, *Scaled Control*). Our data suggest that the number of functional inhibitory synapses is reduced by activity blockade (see above). The fact that mIPSCs are scaled down in a linear manner sug-

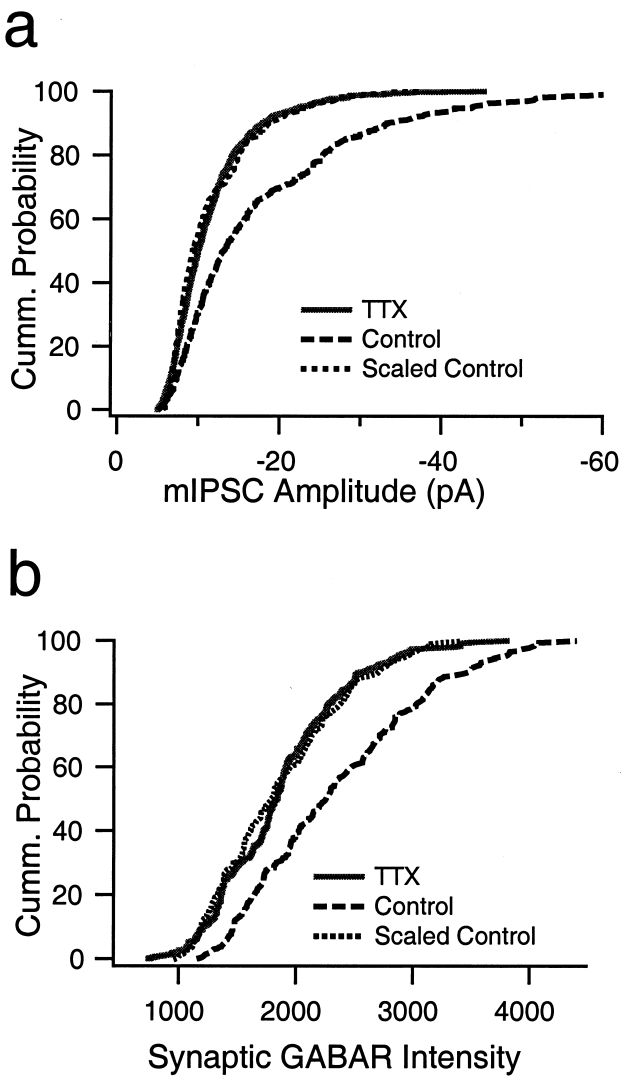

Figure 8. mIPSC amplitude and the fluorescent intensity of synaptic $GABA_AR$ labeling are both reduced in a multiplicative manner by activity blockade. *a*, Cumulative distribution of mIPSC amplitudes from nine control neurons (*dashed line*; 30 events per neuron) and nine neurons treated with TTX for 2 d before recording (*solid line*; 30 events per neuron). Scaling down the control distribution by a factor of 0.46 produced a good fit to the TTX-treated distribution. *b*, Cumulative distribution of the intensity measurements from synaptic $GABA_AR$ puncta from control (*dashed line*; 316 puncta) and neurons treated with TTX for 2 d before recording (*solid line*; 240 puncta). Scaling down the control distribution by a factor of 0.74 produced a good fit to the TTX-treated distribution.

gests that this loss of receptor clusters happens uniformly across the entire amplitude distribution. We performed the same analysis for the distribution of intensities of synaptically localized $GABA_AR$ staining (Fig. 8*b*). Again, TTX treatment shifted the entire distribution of intensities to the left, and plotting the rank-ordered control values against the rank-ordered TTX values generated a relationship that was well fit by a straight line function ($r = 0.99$), with a slope of 0.74 and an intercept of 132. Transforming the control distribution by this equation resulted in a good fit to the TTX data (Fig. 8*b*, *Scaled Control*). These data indicate that both mIPSC amplitudes and the intensity of synaptic staining for $GABA_ARs$ are scaled down by activity in a multiplicative manner.

DISCUSSION

In primate and rodent primary visual cortex, reduced sensory drive leads to a reduction in expression of both GAD and GABA (Hendry and Jones, 1986, 1988; Benson et al., 1991; Benevento et al., 1995), suggesting that the amount of cortical inhibition is regulated by ongoing activity. In previous work, we replicated this phenomenon *in vitro* and demonstrated that activity deprivation reduces the amount of functional inhibition onto cortical pyramidal neurons (Rutherford et al., 1997), but whether this occurred through a change in inhibitory synaptic strength or synapse number was unclear. Here we show that activity blockade reduces the amplitude of mIPSCs, and this is accompanied by a reduction in the number of open channels, as well as the intensity of staining for postsynaptically localized $GABA_ARs$. In addition, the number of synaptically localized puncta immunopositive for $GABA_ARs$ was dramatically reduced. These data suggest that activity regulates inhibition through both changes in the number of receptors clustered at postsynaptic sites and a reduction in the number of functional inhibitory synapses.

A change in mIPSC amplitude could result from a reduced amount of GABA packaged into synaptic vesicles (Frerking et al., 1995), a reduced number of postsynaptic receptors (Nusser et al., 1997, 1998), and/or a change in subunit composition or phosphorylation state of the receptors that modifies single-channel properties (Macdonald and Olsen, 1994; Sieghart, 1995; Cherubini and Conti, 2001). Nonstationary fluctuation analysis indicated that there was no significant change in $GABA_AR$ single-channel conductance, nor were there changes in mIPSC kinetics that might indicate differences in subunit composition. These data suggest that channel properties were unaltered by activity blockade. On the other hand, there was a significant reduction in the number of channels open at the peak of the mIPSC. Peak-scaled fluctuation analysis cannot determine whether a change in the number of open channels is attributable to a change in channel open probability, a change in transmitter concentration in the synaptic cleft, or a reduction in the number of channels clustered at postsynaptic sites (De Koninck and Mody, 1994). Because the intensity of staining for synaptically localized $GABA_ARs$ was reduced in parallel with mIPSC amplitude, our data suggest that the reduction in open channels is produced, at least in part, by a reduction in the number of synaptically localized $GABA_ARs$. Several other studies have now demonstrated that the number of synaptic $GABA_ARs$ can be increased on both a rapid time scale (by insulin application; Wan et al., 1997) and on longer time scales by kindling paradigms (Otis et al., 1994; Nusser et al., 1998). In addition, visual deprivation in primate visual cortex reduces $GABA_AR$ immunoreactivity (Hendry et al., 1994). Together with our data, this suggests that the number of $GABA_ARs$ clustered at synaptic sites, like the number of AMPA receptors (Turrigiano et al., 2000), can be bidirectionally modified in an activity-dependent manner.

Interestingly, the staining intensity for GAD65 also decreased after activity blockade. GAD65 is the isoform of the synthetic enzyme for GABA that is localized to presynaptic terminals (Kaufman et al., 1991). The reduction in GAD65 staining intensity suggests that activity blockade may produce a coordinated set of presynaptic and postsynaptic changes at inhibitory synapses, so that both postsynaptic $GABA_AR$ number and presynaptic GABA synthesis are reduced together. There is evidence that variation in the GABA content of vesicles (Frerking et al., 1995), as well as variation in the number of postsynaptic $GABA_ARs$ (Nusser et al.,

1997, 1998), both contribute to variations in mIPSC amplitude. Although it is not clear that reducing GAD65 levels reduces the GABA content of vesicles, these data do raise the possibility that these two factors cooperate to reduce quantal amplitude after activity blockade.

In addition to reducing the intensity of staining for $GABA_A$Rs at individual synaptic sites, the number of synaptic sites that express detectable levels of $GABA_A$Rs also decreases by ~50%. In agreement with this result, the frequency of mIPSCs was also decreased by ~50%. Some of the decrease in immunohistochemically detectable puncta may be attributable to the reduction in staining intensity, because some puncta may fall below our ability to detect when the intensity of staining is reduced. However, only a small percentage of puncta were close to background intensity levels (which were typically between 500 and 700) (Fig. 8*b*), so the reduction in staining intensity is unlikely to account for more than a few percent of the overall reduction in the density of puncta. Rather, these data suggest that, at some sites, there is a complete loss of postsynaptic $GABA_A$R. At the same time, there is no change in the number of presynaptic contacts that express synapsin, and there is no significant change in the number of presynaptic contacts that express the inhibitory marker GAD65. This suggests that, after 2 d of activity blockade, inhibitory presynaptic contacts may not be anatomically lost but may simply be apposed to postsynaptic sites that no longer express $GABA_A$Rs. Although several *in vitro* and *in vivo* studies have demonstrated a loss of presynaptic inhibitory contacts as a result of activity blockade (Seil and Drake-Baumann, 1994, 2000; Micheva and Beaulieu, 1995; Marty et al., 2000), in these studies activity deprivation was maintained for one to several weeks. It may be that the first event in inhibitory synapse elimination is loss of postsynaptic receptors and that inhibitory presynaptic contacts are only lost after prolonged inactivity.

Because the loss of inhibition produced by 2 d of activity deprivation in cortical cultures is fully reversible (Rutherford et al., 1997), our data suggest that synaptic $GABA_A$R clusters can be lost and regained on a time scale of hours to days. These dynamic changes in the localization and clustering of postsynaptic $GABA_A$Rs are very similar to recent data suggesting that the number of synaptic sites that express detectable levels of AMPA and NMDA receptors can be increased or decreased by long-lasting changes in activity (Craig, 1998). This activity-dependent regulation of the number of sites expressing $GABA_A$Rs may provide a means of postsynaptically "silencing" inhibitory synapses when excitation falls too low, while maintaining the ability to rapidly recruit more inhibition if excitation rises again.

In cortical, hippocampal, and cerebellar cultures, the decrease in inhibition produced by long-lasting activity blockade is mediated by the long-lasting decrease in release of the neurotrophin BDNF (Seil and Drake-Baumann, 1994, 2000; Marty et al., 1996, 2000; Rutherford et al., 1997), although rapid application of higher concentrations of BDNF has been reported to reduce, rather than increase, $GABA_A$R number (Brünig et al., 2001). In cortical cultures, long-lasting decreases in BDNF release is also the signal that scales up the strength of excitatory synapses (Rutherford et al., 1998; Turrigiano, 1999). Reduced BDNF signaling over long timescales may therefore have opposite effects on the trafficking of $GABA_A$Rs and AMPA receptors at inhibitory and excitatory synapses onto cortical pyramidal neurons. Blocking signaling through the high-affinity receptor for BDNF, TrkB, can also cause disassembly of receptor clusters at the neuromuscular junction (Gonzalez et al., 1999), suggesting that BDNF may play a very general role in receptor trafficking and clustering. However, the molecular events that underlie the effects of BDNF on receptor trafficking, and how this neurotrophin can have distinct effects on different classes of synapse onto the same neuron, is still entirely unknown.

The balance between excitation and inhibition in cortical networks can critically influence the level and form of spontaneous activity (Kriegstein et al., 1987; Chagnac-Amitai and Conners, 1989), information transfer through the network (Sillito, 1975; Nelson, 1991; Shadlen and Newsome, 1994, Somers et al., 1995), and experience-dependent synaptic plasticity (Kirkwood and Bear, 1994; Hensch et al., 1998). The ability of activity to change excitatory and inhibitory synaptic strengths in opposite directions suggests that cortical pyramidal neurons can "tune" the relative strengths of excitatory and inhibitory synapses in a dynamic manner, to achieve or maintain particular activity levels. Such "tuning" of synaptic strengths is an essential element in some computational models of persistent activity in recurrent networks (Seung et al., 2000; Wang, 2001). Reciprocal scaling of excitatory and inhibitory synaptic strengths may also serve as an important mechanism that allows neurons to maintain an optimal balance between excitation and inhibition in the face of large changes in synapse number and strength or developmental changes in neuronal structure and excitability.

REFERENCES

Angelotti TP, Macdonald RL (1993) Assembly of $GABA_A$ receptor subunits: $\alpha1\beta2$ and $\alpha1\beta1\gamma2$s subunits produce unique ion channels with dissimilar single-channel properties. J Neurosci 13:1429–1440.

Auger C, Marty A (1997) Heterogeneity of functional synaptic parameters among single release sites. Neuron 19:139–150.

Benevento LA, Bakkum BW, Cohen RS (1995) Gamma-aminobutyric acid and somatostatin immunoreactivity in the visual cortex of normal and dark-reared rats. Brain Res 689:172–182.

Benson DL, Isackson PJ, Gall CM, Jones EG (1991) Differential effects of monocular deprivation on glutamic acid decarboxylase and type II calcium-calmodulin-dependent protein kinase gene expression in the adult monkey visual cortex. J Neurosci 11:31–47.

Brünig I, Penschuck S, Berninger B, Benson J, Fritschy J-M (2001) BDNF reduces miniature inhibitory postsynaptic currents by rapid downregulation of $GABA_A$ receptor surface expression. Eur J Neurosci 13:1320–1328.

Chagnac-Amitai Y, Conners BW (1989) Synchronized excitation and inhibition driven by intrinsically bursting neurons in neocortex. J Neurophysiol 62:1149–1162.

Cherubini E, Conti F (2001) Generating diversity at GABAergic synapses. Trends Neurosci 24:155–162.

Craig AM (1998) Activity and synaptic receptor targeting: the long view. Neuron 21:459–462.

De Koninck Y, Mody I (1994) Noise analysis of miniature IPSCs in adult rat brain slices: properties and modulation of synaptic $GABA_A$ receptor channels. J Neurophysiol 71:1318–1335.

Desai NS, Rutherford LC, Turrigiano GG (1999) Plasticity in the intrinsic excitability of neocortical pyramidal neurons. Nat Neurosci 2:515–520.

Dunning DD, Hoover CL, Soltesz I, Smith MA, O'Dowd DK (1999) $GABA_A$ receptor-mediated miniature postsynaptic currents and α-subunit expression in developing cortical neurons. J Neurophysiol 82:3286–3297.

Frerking M, Borges S, Wilson M (1995) Variation in GABA mini amplitude is the consequence of variation in transmitter concentration. Neuron 15:885–895.

Gonzalez M, Ruggiero FP, Chang Q, Shi YJ, Rich MM, Kraner S, Balice-Gordon RJ (1999) Disruption of TrkB-mediated signaling induces disassembly of postsynaptic receptor clusters at neuromuscular junctions. Neuron 24:567–583.

Hendry SHC, Jones EG (1986) Reduction in number of immunostained GABAergic neurones in deprived-eye dominance columns of monkey area 17. Nature 320:750–753.

Hendry SHC, Jones EG (1988) Activity-dependent regulation of GABA expression in the visual cortex of adult monkeys. Neuron 1:701–712.

Hendry SHC, Huntsman M-M, Viñuela A, Möhler G, de Blas AL, Jones EG (1994) $GABA_A$ receptor subunit immunoreactivity in primate visual cortex: distribution in macaques and humans and regulation by visual input in adulthood. J Neurosci 14:2383–2401.

Hensch TK, Fagiolini M, Mataga N, Stryker MP, Baekkeskov S, Kash SF (1998) Local GABA circuit control of experience-dependent plasticity in developing visual cortex. Science 282:1504–1508.

Kaufman DL, Houser CR, Topbin AJ (1991) Two forms of the gamma-aminobutryic acid synthetic enzyme glutamate decarboxylase have distinct intraneuronal distributions and cofactor interactions. J Neurochem 56:720–723.

Kirkwood A, Bear MF (1994) Hebbian synapses in visual cortex. J Neurosci 14:1634–1645.

Kriegstein AR, Suppes T, Prince DA (1987) Cellular and synaptic physiology and epileptogenesis of developing rat neocortical neurons in vitro. Dev Brain Res 34:161–171.

Lissen DV, Gomperts SN, Carroll RC, Christine CW, Kalman D, Kitamura M, Hardy S, Nicoll RA, Malenka RC, von Zastrow M (1998) Activity differentially regulates the surface expression of synaptic AMPA and NMDA glutamate receptors. Proc Natl Acad Sci USA 95:7097–7102.

Macdonald RL, Olsen RW (1994) $GABA_A$ receptor channels. Annu Rev Neurosci 17:569–602.

Marty S, Berninger B, Carroll P, Thoenen H (1996) GABAergic stimulation regulates the phenotype of hippocampal interneurons through the regulation of brain-derived neurotrophic factor. Neuron 16:565–570.

Marty S, Wehrle R, Sotelo C (2000) Neuronal activity and brain-derived neurotrophic factor regulate the density of inhibitory synapses in organotypic slice cultures of postnatal hippocampus. J Neurosci 20:8087–8095.

Micheva KD, Beaulieu C (1995) An anatomical substrate for experience-dependent plasticity of the rat barrel field cortex. Proc Natl Acad Sci USA 92:11834–11838.

Nelson SB (1991) Temporal interactions in the cat visual system. III. Pharmacological studies of cortical suppression suggest a presynaptic mechanism. J Neurosci 11:369–380.

Nusser Z, Cull-Candy S, Farrant M (1997) Differences in synaptic $GABA_A$ receptor number underlie variation in GABA mini amplitude. Neuron 19:697–709.

Nusser Z, Hajos N, Somogyi P, Mody I (1998) Increased number of synaptic $GABA_A$ receptors underlies potentiation at hippocampal inhibitory synapses. Nature 395:172–177.

O'Brien RJ, Kambol S, Ehlers MD, Rosen KR, Kischback GD, Huganir RL (1998) Activity-dependent modulation of synaptic AMPA receptor accumulation. Neuron 21:1067–1078.

Otis TS, De Koninck Y, Mody I (1994) Lasting potentiation of inhibition is associated with an increased number of gamma-aminobutyric acid type A receptors activated during miniature inhibitory postsynaptic currents. Proc Natl Acad Sci USA 91:7698–7702.

Rutherford LC, Dewan A, Lauer HM, Turrigiano GG (1997) BDNF mediates the activity-dependent regulation of inhibition in neocortical cultures. J Neurosci 17:4527–4536.

Rutherford LC, Nelson SB, Turrigiano GG (1998) Opposite effects of BDNF on the quantal amplitude of pyramidal and interneuron excitatory synapses. Neuron 21:521–530.

Seil FJ, Drake-Baumann R (1994) Reduced cortical inhibitory synaptogenesis in organotypic cerebellar cultures developing in the absence of neuronal activity. J Comp Neurol 342:366–377.

Seil FJ, Drake-Baumann R (2000) TrkB receptor ligands promote activity-dependent inhibitory synaptogenesis. J Neursci 20:5367–5373.

Seung HS, Lee DD, Reis BY, Tank DW (2000) Stability of the memory of eye position in a recurrent network of conductance-based model neurons. Neuron 26:259–271.

Shadlen MN, Newsome WT (1994) Noise, neural codes and cortical organization. Curr Opin Neurobiol 4:568–579.

Sieghart W (1995) Structure and pharmacology of γ-aminobutyric $acid_A$ receptor subtypes. Pharmacol Rev 47:181–234.

Sillito AM (1975) The contribution of inhibitory mechanisms to the receptive field properties of neurones in the striate cortex of the cat. J Physiol (Lond) 250:305–329.

Somers DC, Nelson SB, Sur M (1995) An emergent model of orientation selectivity in cat visual cortical simple cells. J Neurosci 15:5448–5465.

Traynelis SG, Sliver RA, Cull-Candy SG (1993) Estimated conductance of glutamate receptor channels activated during EPSCs at the cerebellar mossy fiber-granule cell synapse. Neuron 11:279–289.

Turrigiano GG (1999) Homeostatic plasticity in neuronal networks: the more things change, the more they stay the same. Trends Neurosci 22:221–228.

Turrigiano GG, Nelson SB (2000) Hebb and homeostasis in neuronal plasticity. Curr Opin Neurobiol 10:358–364.

Turrigiano GG, Leslie KR, Desai NS, Rutherford LC, Nelson SB (1998) Activity-dependent scaling of quantal amplitude in neocortical pyamidal neurons. Nature 391:892–895.

Wan Q, Xiong ZG, Man HY, Ackerley CA, Braunton J, Lu WY, Becker LE, MacDonald JF, Wang YT (1997) Recruitment of functional GABAa receptors to postsynaptic domains by insulin. Nature 388:686–690.

Wang X-J (2001) Synaptic reverberation underlying mnemonic persistent activity. Trends Neurosci 24:455–463.

Watt A, van Rossum M, MacLeod K, Nelson SB, Turrigiano GG (2000) Activity co-regulates quantal AMPA and NMDA currents at neocortical synapses. Neuron 26:659–670.

Wierenga CJ, Wadman WJ (1999) Miniature inhibitory postsynaptic currents in CA1 pyramidal neurons after kindling epileptogenesis. J Neurophysiol 82:1352–1362.